

Electronic states of domain walls in commensurate charge density wave ground state and mosaic phase in 1*T*-TaS_2

Yan Li(李彦), Yao Xiao(肖遥), Qi Zheng(郑琦), Xiao Lin(林晓), Li Huang(黄立), and Hong-Jun Gao(高鸿钧)
Citation: Chin. Phys. B, 2023, 32 (**7**): 077101. DOI: 10.1088/1674-1056/accd4f
Journal homepage: http://cpb.iphy.ac.cn; http://iopscience.iop.org/cpb

What follows is a list of articles you may be interested in

Flat band in hole-doped transition metal dichalcogenide observed by angle-resolved photoemission spectroscopy

Zilu Wang(王子禄), Haoyu Dong(董皓宇), Weichang Zhou(周伟昌), Zhihai Cheng(程志海), and Shancai Wang(王善才)
Chin. Phys. B, 2023, 32 (**6**): 067103. DOI: 10.1088/1674-1056/acc7f9

Charge density wave states in phase-engineered monolayer VTe_2

Zhi-Li Zhu(朱知力), Zhong-Liu Liu(刘中流), Xu Wu(武旭), Xuan-Yi Li(李轩熠), Jin-An Shi(时金安), Chen Liu(刘晨), Guo-Jian Qian(钱国健), Qi Zheng(郑琦), Li Huang(黄立), Xiao Lin(林晓), Jia-Ou Wang(王嘉欧), Hui Chen(陈辉), Wu Zhou(周武), Jia-Tao Sun(孙家涛), Ye-Liang Wang(王业亮), and Hong-Jun Gao(高鸿钧)
Chin. Phys. B, 2022, 31 (**7**): 077101. DOI: 10.1088/1674-1056/ac6739

Effect of strain on charge density wave order in α-U

Liuhua Xie(谢刘桦), Hongkuan Yuan(袁宏宽), and Ruizhi Qiu(邱睿智)
Chin. Phys. B, 2022, 31 (**6**): 067103. DOI: 10.1088/1674-1056/ac4f4d

Tri-hexagonal charge order in kagome metal CsV_3Sb_5 revealed by ^{121}Sb nuclear quadrupole resonance

Chao Mu(牟超), Qiangwei Yin(殷蔷薇), Zhijun Tu(涂志俊), Chunsheng Gong(龚春生), Ping Zheng(郑萍), Hechang Lei(雷和畅), Zheng Li(李政), and Jianlin Luo(雒建林)
Chin. Phys. B, 2022, 31 (**1**): 017105. DOI: 10.1088/1674-1056/ac422c

Direct observation of melted Mott state evidenced from Raman scattering in 1T-TaS_2 single crystal

Qing Hu(胡庆), Cong Yin(尹聪), Leilei Zhang(张雷雷), Li Lei(雷力), Zhengshang Wang(王正上), Zhiyu Chen(陈志禹), Jun Tang(唐军), Ran Ang(昂然)
Chin. Phys. B, 2018, 27 (**1**): 017104. DOI: 10.1088/1674-1056/27/1/017104

RAPID COMMUNICATION

Electronic states of domain walls in commensurate charge density wave ground state and mosaic phase in 1*T*-TaS_2

Yan Li(李彦)[1,2], Yao Xiao(肖遥)[1,2], Qi Zheng(郑琦)[1,2], Xiao Lin(林晓)[2,†], Li Huang(黄立)[1,2,‡], and Hong-Jun Gao(高鸿钧)[1,2]

[1] *Beijing National Center for Condensed Matter Physics and Institute of Physics, Chinese Academy of Sciences, Beijing* 100190, *China*
[2] *School of Physical Sciences, University of Chinese Academy of Sciences, Beijing* 100490, *China*

(Received 12 March 2023; revised manuscript received 10 April 2023; accepted manuscript online 16 April 2023)

Domain walls (DWs) in the charge-density-wave (CDW) Mott insulator 1*T*-TaS_2 have unique localized states, which play an important role in exploring the electronic properties of the material. However, the electronic states in DWs in 1*T*-TaS_2 have not been clearly understood, mostly due to the complex structures, phases, and interlayer stacking orders in the DW areas. Here, we explored the electronic states of DWs in the large-area CDW phase and mosaic phase of 1*T*-TaS_2 by scanning tunneling spectroscopy. Due to the different densities of DWs, the electronic states of DWs show distinct features in these phases. In the large area CDW phase, both the domain and the DWs (DW1, DW2, DW4) have zero conductance at the Fermi level; while in the mosaic phase, they can be metallic or insulating depending on their environments. In areas with a high density of DWs, some electronic states were observed both on the DWs and within the domains, indicating delocalized states over the whole region. Our work contributes to further understanding of the interplay between CDW and electron correlations in 1*T*-TaS_2.

Keywords: 1*T*-TaS_2, scanning tunneling spectroscopy, domain walls, charge density wave

PACS: 71.45.Lr, 73.22.–f, 68.37.Ef, 75.60.Ch **DOI:** 10.1088/1674-1056/accd4f

Domain walls (DWs) in 1*T*-TaS_2 have great influences on the electronic properties of the material,[1–10] thus have always been one of the key research directions in this field. Although the strength of the electron–electron correlation is similar inside the intrinsic 1*T*-TaS_2 domains, the correlation strength decreases where DWs exist.[6] The interplay between charge density wave (CDW) and electron correlation renders rich physics in the electronic states of DWs.[1–3,6,11,12]

Intensive experimental and theoretical studies have demonstrated that DWs with different atomic structures have different electronic states, ranging from insulating to conductive.[3,6,13,14] Furthermore, the density of DWs also affects the electronic states of the system.[6,15] For example, 1*T*-TaS_2 will change from a Mott insulator in commensurate CDW (CCDW) phase to a metal when the density of DWs increases significantly.[14,16,17] In the CCDW phase, a voltage pulse across the tip–sample junction could create DWs in high density, resulting in a mosaic state that can be metallic.[2] Therefore, the electronic states of DWs are not only determined by the atomic structures, but also by the density of the DWs. The complexity of this hinders the understanding of the electronic states in DWs, which calls for more thorough work to investigate DWs of different types in different densities.

Here, we present the scanning tunneling spectroscopy (STS) results on the DWs of 1*T*-TaS_2 in areas with different DW densities, namely DWs between large CCDW domains, between a large and a small CCDW domain, and in the mosaic phase. We found that for DWs between large domains, the STS on both DWs and the domain edges (DEs), the nearest intact stars of David (SDs) on the two sides of the DWs have a V-shaped gap with no spectral weight at E_F. For DWs between a large and a small CCDW domain, the DEs have a finite spectral weight at E_F, indicating a metallic state, while the DWs remain insulating. For DWs in the mosaic phase, the domains can be metallic or insulating. The electronic states on the domain edges and inside the domains tend to have the same states. The DWs show states suppression near E_F and share some similar states with the domains.

Our scanning tunneling microscopy/spectroscopy (STM/S) measurements were carried out in a Createc STM system in ultrahigh vacuum condition, with a base pressure better than 5×10^{-1} mbar, at a low-temperature of 4.3 K. The 1*T*-TaS_2 single crystal was purchased from HQ Graphene. The samples with pre-glued aluminum rods were cleaved at room temperature in the UHV chamber, and then transferred to the precooled STM head immediately. STM images were acquired in the constant current mode.

The 1*T*-TaS_2 has a commensurate charge density wave (CCDW) ground state when the temperature is below 180 K, in which the triangular-latticed Ta atoms deform into SDs where every 12 Ta atoms contract towards a central Ta site, forming a $\sqrt{13}\times\sqrt{13}$ superlattice[18–21] (Fig. 1(a)). The CCDW super-

†Corresponding author. E-mail: xlin@ucas.ac.cn
‡Corresponding author. E-mail: lhuang@iphy.ac.cn

© 2023 Chinese Physical Society and IOP Publishing Ltd

structure is accompanied by electronic modulations, leaving only one conduction electron per SDs.[22–26] Strong electron correlations between SD clusters further lead to a Mott insulating ground state.[27–32] The SDs have shifted center positions in different domains. The merge of two domains results in a domain wall (DW) that consists of one or two incomplete lines of SDs.[1,13] Judging from the atomic structure, there are 12 possible types of DWs, each of which possesses unique electronic structures.[3,13] In the CCDW phase, DWs usually locate between large-are domains (Fig. 1(b)). While in the mosaic phase, the DWs have high density, resulting in domains with very small areas (Fig. 1(c)).

Figure 2(a) shows an STM image of the CCDW region with a DW marked by two parallel black dashed lines. The domains (marked by D) have triangular-latticed SDs, while the DW has a much lower contrast in the STM image at this scanning parameter. DWs in $1T$-TaS_2 can be classified into 12 types, out of which only 3 types of DWs, DW1, DW2 and DW4, have high frequency of occurrence,[6,13] as shown by the STM images in Figs. 2(b)–2(d), respectively. The superimposed lilac and pink SD models illustrate the relative shifts of the SD centers in the neighboring domains. Among the three DWs, DW1 and DW4 consist of only one column of incomplete SDs, while DW2 is composed of two columns of incomplete SDs, as indicated by the black dashed lines in each figure. The DEs, which are the nearest complete SDs on the two sides of the DWs, are highlighted by the white dashed lines.

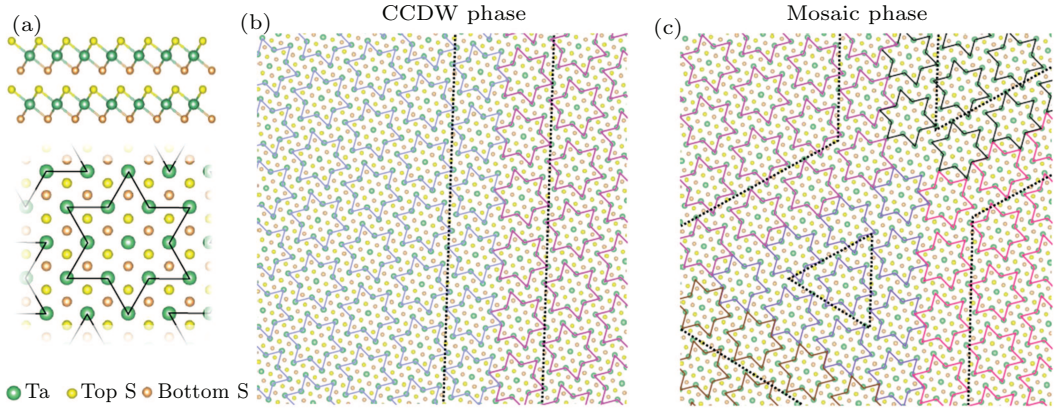


Fig. 1. Schematic of atomic structure of $1T$-TaS_2. (a) Side view and top-view atomic structure of $1T$-TaS_2. The superimposed black lines show the SD. (b) The atomic structure of DW in the CCDW phase. The two domains are superimposed with lilac and pink SD superlattices. The DW is marked by two parallel black dashed lines. (c) The atomic structure of DWs in the mosaic phase. Different domains are superimposed with SD superlattices with different colors. The DWs are marked by parallel black dashed lines.

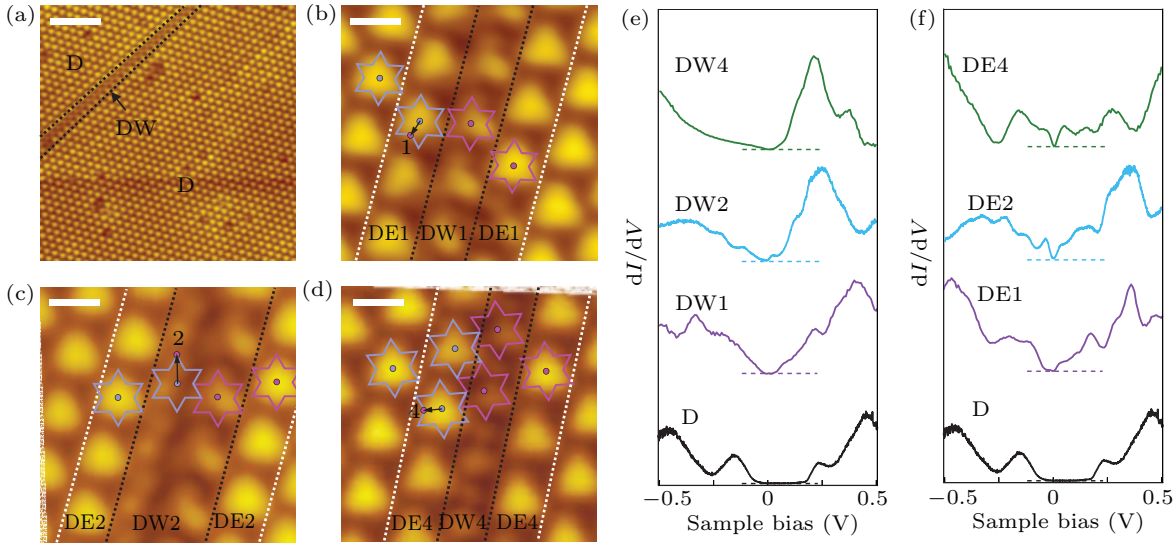


Fig. 2. STM images and STS on DWs between large domains in $1T$-TaS_2. (a) Large-area STM image of CCDW domains and a DW in the upper left part of the image. The black dashed lines highlight the position of the DW. (b)–(d) Zoom-in STM images of DW1, DW2, DW4, superimposed with the schematic lilac and pink DS superlattice. Domain walls with deformed SDs are marked by dashed black lines. Domain edges with complete SDs nearest to the DWs on both sides are drawn out by the white dashed lines. The black arrows show the vectors of the relative phase shifts of the CDW pattern between the two domains. (e) $\mathrm{d}I/\mathrm{d}V$ spectra taken on the CCDW domain region (black), DW1 (purple), DW2 (blue) and DW4 (green). The horizontal dashed lines represent the zero spectral weight of each STS. The STS curves are vertically shifted for clarity. (f) $\mathrm{d}I/\mathrm{d}V$ spectra taken on the CCDW domain region (black), DE1 (purple), DE2 (blue) and DE4 (green). STM scanning parameters in (a)–(d): bias voltage applied to the sample $V_S = -1$ V, tunneling current $I_t = 10$ pA. STS parameters in (e) and (f): $V_S = -0.1$ V, $I_t = 10$ pA, the modulated output voltage from the lock-in amplifier $V_{mod} = 5$ mV, modulation frequency $f_{mod} = 761$ Hz. Scale bars: 8 nm in (a) and 1 nm in (b)–(d).

The dI/dV spectra taken on both DWs and DEs in Figs. 2(e) and 2(f) show a V-shaped gap instead of a Mott gap around the Fermi level. The incomplete SDs in DWs are accompanied by the changes of the onsite Coulomb repulsion energy U, therefore reduce the width of the Mott gap.[6,8] Once breaking the long range CDW order, the Mott gap of DWs turns into a V-shaped gap, because the peaks corresponding to the upper Hubbard band (UHB) and the lower Hubbard band (LHB) become broader and closer to the Fermi level. For all the DWs and DEs in Fig. 2, the spectral weight at the Fermi level is zero. The dI/dV spectra taken at the second nearest SD neighbors to the DWs returns to a normal Mott gap, indicating that the electronic states of these SDs are no longer subject to the influence of DWs.

In the DW regions, the incomplete SDs can no longer trap the unpaired 5d electrons at the center of SD, which leads to the weakening of Coulomb interaction together with increasing of electron hopping between adjacent SDs. Therefore, the lower Hubbard band and the upper Hubbard band shift towards the Fermi level, resulting in Mott collapse with a V-shaped gap on the DWs. For the DE regions, although the SDs are intact, they are still affected by the delocalized 5d electrons in the DW regions, rendering a similar V-shaped gap as that on the DWs.

Next, we created a mosaic phase by applying voltage pulses from the STM tip.[1,2,4] Since the periodicity is significantly broken in the mosaic region, the electronic states of DWs and domains can be fairly complicated.[1,2,4,9] We first focus on the edge area of the mosaic region, where the DWs are relatively sparse, as shown in the large-area STM image in Fig. 3(a). The black dashed lines mark the edges of a large domain (D_L) and a triangular shaped small domain (D_S), which are separated by a DW2. The zoom-in STM image in Fig. 3(b) shows the DW2 (marked by the parallel black dashed lines), the domain edges to the D_L and D_S side (DE_L and DE_S, by white dashed lines), and the two domains.

The D_L has similar electronic states as those in large-area CCDW domains, as shown by the pink curve in Fig. 3(c). However, the STS of D_S has a metallic V-shape around the Fermi level (green curve in Fig. 3(c)), which is a feature for small domains in the mosaic region due to the reduction of electron correlation as reported by published works.[1,2] Furthermore, there are additional free electrons released by the Mott collapse to make the metallic state, indicating the electron correlation in D_S should be even weaker than that in the DWs in large-area CCDW regions as shown in Fig. 2. Similar to the STS of DW2 in Fig. 2, there is also a V-shaped gap in the dI/dV spectra of DW2 in Fig. 3(c) (the red curve), whereas the states at the unoccupied energies look very different. For the domain edges though, the STS on both DE_L and DE_S have a V-shape with finite spectral weight around the Fermi level, which is different from the case in large-area CCDW where the DE2 is insulating. The higher density of domain walls leads to weaker electronic correlations compared to the large-area CCDW regions, resulting in more delocalized 5d electrons contributing to the metallic state on the domain edges.

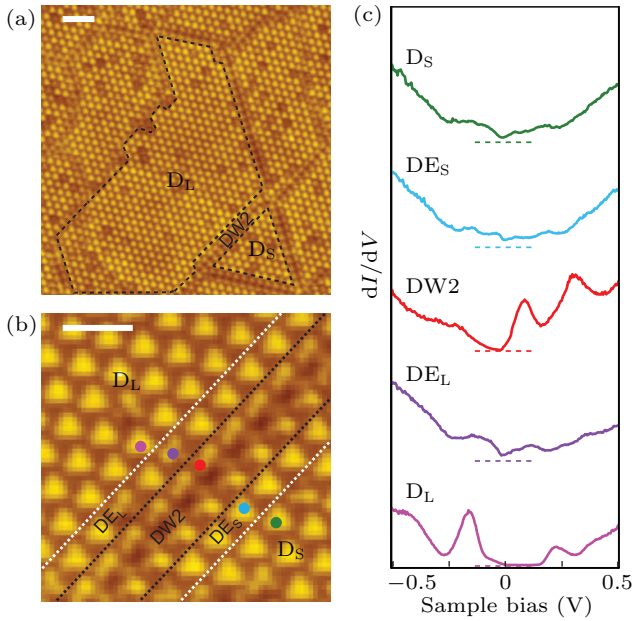


Fig. 3. STM images and STS on DW2 in a mosaic region with relatively sparse DWs in 1T-TaS_2. (a) Large-area STM image of an area composed of mosaic domains separated by sparse domain walls. Superimposed black dashed lines enclose two typical domains. (b) Zoom-in STM image of the same DW2 as highlighted in (a). DW2 is circled by the parallel black dashed lines. Domain edges with complete SDs nearest to the deformation SDs on both sides are drawn out by the white dashed lines. The colorful circles mark the positions where dI/dV spectra are taken. (c) dI/dV spectra taken at D_L (pink), D_S (green), the domain edge near the large domain (DE_L, purple), the domain edge near the small domain (DE_S, blue) and DW2 (red). The horizontal dashed lines represent zero spectral weight of each STS. The STS curves are vertically shifted for clarity. STM scanning parameters in (a) and (b): $V_S = -1$ V, $I_t = 10$ pA. STS parameters in (c): $V_S = -0.1$ V, $I_t = 10$ pA, $V_{mod} = 5$ mV, $f_{mod} = 761$ Hz. Scale bars: 5 nm in (a) and 2.5 nm in (b).

For the mosaic region with intensive DWs, the long-range ordered CCDW pattern is divided into small pieces of polygons separated by DWs, as shown by the black dashed lines in Fig. 4(a). We have performed STS characterizations on multiple DWs and domains. For domains, the electron states are V-shaped, like the ones on the DWs or DEs in the large-area CCDW region. We noticed that the spectral weight at the Fermi level varies in different domains. For example, the light blue curve (domain D) in Fig. 4(b) is insulating, while the dark blue curve (domain D′) is metallic. Some published works indicate that dense DWs not only change the localized Coulomb repulsion, but also change the bandwidth.[7,33–36] Also, the vertical stacking orders of different domains may contribute to the varied electronic states.[4,35]

The STS taken at DW1, DW2,8, and DW4 all display a V-shape feature (the green, red and purple curves in Fig. 4(b)), among which DW4 has more spectral weight at the Fermi level, whereas the other DWs have near zero conductance near the Fermi level. What's more, the spectra taken at both DWs and domains of the mosaic region seem to share some similar states at −40 meV, +50 meV and +200 meV, as indicated by the orange dotted vertical lines in Fig. 4(b), although the relative intensity of these peaks varies on different sites. There-

fore, we can infer that in the mosaic area, the influence of breaking the long-range CDW order spreads from the original one or two columns of DW SDs to the entire mosaic region.

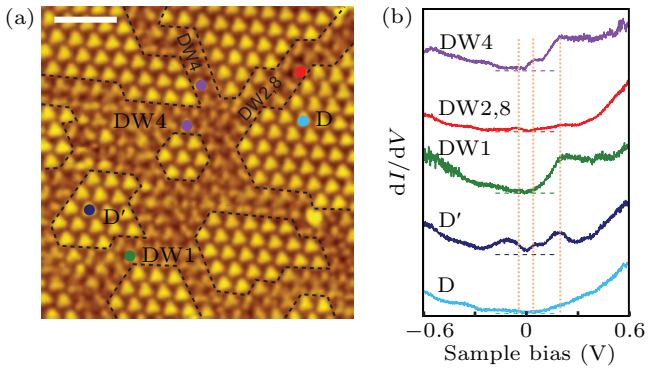


Fig. 4. STM image and STS on DWs in a mosaic region in 1T-TaS_2. (a) STM image of mosaic domains separated by dense DWs. The black dashed lines show the edges of the domains. The types of DWs are marked in the figure. The colorful circles show the positions where the dI/dV spectra were taken. (b) dI/dV spectra taken in domains (light blue and dark blue), DW1 (green), DW2,8 (red) and DW4 (purple). The horizontal dashed lines represent zero spectral weight of each STS, while the vertical dotted orange lines mark peaks shared by several STS. The STS curves are vertically shifted for clarity. STM scanning parameters in (a): $V_S = -1$ V, $I_t = 10$ pA. STS parameters in (b): $V_S = -0.1$ V, $I_t = 10$ pA, $V_{mod} = 5$ meV, $f_{mod} = 761$ Hz. Scale bar: 4 nm.

Compared with previous works on mosaic phase in which the whole region shows a metallic state,[1,2] our work discovers that there are also insulating regions both within domains and on DWs in the mosaic phase. With the high density of DWs, the delocalization of 5d electrons in the DWs has strong influence on the intact SDs, resulting in a complete Mott collapse not only on DWs and DEs, but also within the domains. Some studies suggest that the additional free electrons released by Mott collapse may form quasi-particle energy bands that split into bonding and anti-bonding states,[6] which may be a possible reason for the insulating areas in the mosaic phase observed in this work. However, due to the complexity of the type of DWs and the size of domains, further investigations are still needed to elucidate the mechanism for the electronic states in the mosaic phase.

In conclusion, we demonstrated that the large-area CCDW phase in *1T*-TaS_2 has a zero conductance around the Fermi level both in domains and at DW1, DW2, DW4 and their DEs. However, in the mosaic region, the electronic states are very complicated. Besides the shared feature of a V-shaped spectra around the Fermi level, the domains, DWs, and DEs can be metallic or insulating, which seem to be highly affected by the neighboring environment. Our work provides detailed information on the electronic states in both large-area CCDW and mosaic phases, which may contribute to better understanding of the interplay of CDW and electron correlations in *1T*-TaS_2.

Acknowledgements

Project supported by the National Key Research and Development Project of China (Grant No. 2019YFA0308500), the National Natural Science Foundation of China (Grant No. 61888102), and the Chinese Academy of Sciences (Grant Nos. XDB30000000 and YSBR-003).

References

[1] Cho D, Cheon S, Kim K S, Lee S H, Cho Y H, Cheong S W and Yeom H W 2016 *Nat. Commun.* **7** 10453
[2] Ma L, Ye C, Yu Y, Lu X F, Niu X, Kim S, Feng D, Tomanek D, Son Y W, Chen X H and Zhang Y 2016 *Nat. Commun.* **7** 10956
[3] Cho D, Gye G, Lee J, Lee S H, Wang L, Cheong S W and Yeom H W 2017 *Nat. Commun.* **8** 392
[4] Salzmann B, Hujala E, Witteveen C, Hildebrand B, Berger H, Rohr F, Nicholson C and Monney C 2023 *Phys. Rev. Mater.* **7** 064005
[5] Yao Q, Park J W, Oh E and Yeom H W 2021 *Nano Lett.* **21** 9699
[6] Skolimowski J, Gerasimenko Y and Zitko R 2019 *Phys. Rev. Lett.* **122** 036802
[7] Butler C J, Yoshida M, Hanaguri T and Iwasa Y 2020 *Nat. Commun.* **11** 2477
[8] Karpov P and Brazovskii S 2018 *Sci. Rep.* **8** 4043
[9] Zhang W, Gao J, Cheng L, Bu K, Wu Z, Fei Y, Zheng Y, Wang L, Li F, Luo X, Liu Z, Sun Y and Yin Y 2022 *npj Quantum Mater.* **7** 8
[10] Zong A, Shen X, Kogar A, Ye L, Marks C, Chowdhury D, Rohwer T, Freelon B, Weathersby S, Li R, Yang J, Checkelsky J, Wang X and Gedik N 2018 *Sci. Adv.* **4** eaau5501
[11] Cho D, Cho Y H, Cheong S W, Kim K S and Yeom H W 2015 *Phys. Rev. B* **92** 085132
[12] Sayers C J, Hedayat H, Ceraso A, Museur F, Cattelan M, Hart L S, Farrar L S, Dal Conte S, Cerullo G, Dallera C, Da Como E and Carpene E 2020 *Phys. Rev. B* **102** 161105
[13] Park J W, Lee J and Yeom H W 2021 *npj Quantum Mater.* **6** 32
[14] Park J W, Cho G Y, Lee J and Yeom H W 2019 *Nat. Commun.* **10** 4038
[15] Fei Y, Wu Z, Zhang W and Yin Y 2022 *AAPPS Bulletin* **32** 20
[16] Wen W, Dang C and Xie L 2019 *Chin. Phys. B* **28** 58504
[17] Wu X L and Lieber C M 1990 *Phys. Rev. Lett.* **64** 1150
[18] Giambattista B, Slough C G, McNairy W W and Coleman R V 1990 *Phys. Rev. B* **41** 10082
[19] Kazuo N and Hiroyuki S 1984 *J. Phys. Soc. Jpn.* **53** 1103
[20] Rossnagel K and Smith N V 2006 *Phys. Rev. B* **73** 073106
[21] Thomson R E, Walter U, Ganz E, Clarke J, Zettl A, Rauch P and DiSalvo F J 1988 *Phys. Rev. B* **38** 10734
[22] Liu L, Yang H, Huang Y, Song X, Zhang Q, Huang Z, Hou Y, Chen Y, Xu Z, Zhang T, Wu X, Sun J, Huang Y, Zheng F, Li X, Yao Y, Gao H J and Wang Y 2021 *Nat. Commun.* **12** 1978
[23] Yang H, Zhang T, Huang Z, Chen Y, Song X, Hao X, Yang H, Wu X, Zhang Y, Liu L, Gao H J and Wang Y 2022 *ACS Nano* **16** 1332
[24] Chen Y, Liu L, Song X, Yang H, Huang Z, Zhang T, Yang H, Gao H J and Wang Y 2022 *2D Mater.* **9** 014007
[25] Huang Z, Song X, Chen Y, Yang H, Yuan P, Ma H, Qiao J, Zhang Y, Sun J, Zhang T, Huang Y, Liu L, Gao H J and Wang Y 2022 *J. Phys. Chem. Lett.* **13** 1901
[26] Liu L, Song X, Dai J, Yang H, Chen Y, Huang X, Huang Z, Ji H, Zhang Y, Wu X, Sun J T, Zhang Q, Zhou J, Huang Y, Qiao J, Ji W, Gao H J and Wang Y 2023 *ACS Nano* **17** 2702
[27] Fazekas P and Tosatti E 1980 *Physica B+C* **99** 183
[28] Rossnagel K 2011 *J. Phys. Condens. Matter* **23** 213001
[29] Pillo T, Hayoz J, Berger H, Fasel R, Schlapbach L and Aebi P 2000 *Phys. Rev. B* **62** 4277
[30] Clerc F, Battaglia C, Bovet M, Despont L, Monney C, Cercellier H, Garnier M G, Aebi P, Berger H and Forró L 2006 *Phys. Rev. B* **74** 155114
[31] Sipos B, Kusmartseva A F, Akrap A, Berger H, Forro L and Tutis E 2008 *Nat. Mater.* **7** 960
[32] Song X, Liu L, Chen Y, Yang H, Huang Z, Hou B, Hou Y, Han X, Yang H, Zhang Q, Zhang T, Zhou J, Huang Y, Zhang Y, Gao H J and Wang Y 2022 *Nat. Commun.* **13** 1843
[33] Wang Y D, Yao W L, Xin Z M, Han T T, Wang Z G, Chen L, Cai C, Li Y and Zhang Y 2020 *Nat. Commun.* **11** 4215
[34] Lee S H, Goh J S and Cho D 2019 *Phys. Rev. Lett.* **122** 106404
[35] Wu Z, Bu K, Zhang W, Fei Y, Zheng Y, Gao J, Luo X, Liu Z, Sun Y-P and Yin Y 2022 *Phys. Rev. B* **105** 035109
[36] Petocchi F, Nicholson C W, Salzmann B, Pasquier D, Yazyev O V, Monney C and Werner P 2022 *Phys. Rev. Lett.* **129** 016402